http://dx.doi.org/10.18623/rvd.v23.6320

ELASTO-NANO-MECHANICAL CHARACTERIZATION OF BIO-DERIVED NANO-$CACO_3$-REINFORCED SUSTAINABLE ECO-FRIENDLY CONCRETES FOR CO_2 EMISSION REDUCTION: FREE VIBRATION ANALYSIS OF RAFT FOUNDATIONS

CARACTERIZAÇÃO ELASTO-NANOMECÂNICA DE BETÕES SUSTENTÁVEIS E ECOLÓGICOS REFORÇADOS COM NANO-$CACO_3$ DE ORIGEM BIOLÓGICA PARA A REDUÇÃO DAS EMISSÕES DE CO_2: ANÁLISE DE VIBRAÇÃO LIVRE DE FUNDAÇÕES EM LAJE

Article received on: 1/2/2026
Article accepted on: 4/1/2026

Mohammedi Mohammed Nourelislam*
*Laboratory of Advanced Structures and Materials in Civil Engineering and Public Works, Sidi Bel Abbes, Algeria
Orcid: https://orcid.org/0009-0009-1324-4366
nourelislam.mohammedi@dl.univ-sba.dz

Altarhouni Lutfiyah Abraham Mohammed**
**Faculty of Natural Resources, University of Zawiya, Ajilat, Libya
Orcid: https://orcid.org/0009-0005-3217-8094
l.altarhouni@zu.edu.ly

Alsbhawy Mohamed Abdouslam Aboubakar***
***Department of Civil and Environmental Engineering, Faculty of Engineering, University of Sebha, Sebha, Libya
Orcid: https://orcid.org/0009-0005-1973-5255
mohamed.a.aboubakar@gmail.com

Benfrid Abdelmoutalib****
******Djillali Liabès University, Sidi Bel Abbès, Algeria
Orcid: https://orcid.org/0009-0007-8171-1654
benfridabdelmoutalib2050@gmail.com

Benatta Mohamed Atef*
*Laboratory of Advanced Structures and Materials in Civil Engineering and Public Works, Sidi Bel Abbes, Algeria
Orcid: https://orcid.org/0009-0007-5854-9054
bematif@gmail.com

Bachir Bouiadjra Mohammed*
*Laboratory of Advanced Structures and Materials in Civil Engineering and Public Works, Sidi Bel Abbes, Algeria
Orcid: https://orcid.org/0009-0008-4814-6187
mohamedbachirbouiadjra@gmail.com

Krour Baghdad*
*Laboratory of Advanced Structures and Materials in Civil Engineering and Public Works, Sidi Bel Abbes, Algeria
Orcid: https://orcid.org/0000-0002-8265-9807
krour.bag@gmail.com

The authors declare that there is no conflict of interest

Abstract
Natural waste products—such as eggshells, animal bones, and marine deposits—serve as sustainable sources for nano-calcium carbonate ($CaCO_3$) extraction. Valorizing these nanoparticles for concrete reinforcement is crucial for developing durable, high-performance infrastructure. This study adopts a two-fold approach: first, the Hashin–Shtrikman model is utilized to predict the nanomechanical properties of bio-reinforced eco-concrete; second, the free vibration response of a raft foundation is analyzed using FSDT and HSDT frameworks. Findings reveal that nano-$CaCO_3$ incorporation not only optimizes nanomechanical characteristics but also significantly improves structural stiffness and vibrational stability.

Keywords: Eco-Concrete. Nano-Calcium Carbonate (Nano-$Caco_3$). Bio-Sourced Nanoparticles. Hashin–Shtrikman Model. Free Vibration Analysis. Raft Foundation.

Resumo
Produtos naturais descartados, incluindo cascas de ovos e depósitos marinhos, são fontes sustentáveis de Nano-$CaCO_3$. Este trabalho investiga o uso dessas nanopartículas no reforço de concretos ecológicos através de uma metodologia analítica dupla: a aplicação do modelo de Hashin-Shtrikman para caracterização nanomecânica e a análise dinâmica de um radier baseada nas teorias FSDT e HSDT. Os achados indicam que a adição de nano-CaCO3 potencializa o desempenho mecânico do material e aumenta a eficiência estrutural frente a vibrações livres.

Palavras-chave: *Ecoconcreto. Nanocarbonato de Cálcio (Nano-$Caco_3$). Nanopartículas Biosourçadas. Modelo de Hashin–Shtrikman. Análise de Vibração Livre. Radier de Fundação.*

1 INTRODUCTION

Nanoparticle technology has experienced rapid development in recent years, significantly influencing the field of material reinforcement. Concrete, as one of the most widely used traditional construction materials, has greatly benefited from these advancements. Investigating its behavior at the nanoscale has become essential, particularly in understanding how the incorporation of nanoparticles—either dispersed randomly or arranged periodically—modifies its mechanical performance. Several studies have explored this topic. Harrat et al. analyzed the influence of nano-silica agglomeration using the Voigt homogenization model [1]. Chatbi et al. investigated the agglomeration of reinforcements within slab structures [2]. Benfrid et al. applied the Eshelby model to evaluate the thermal tensor of panels containing nano-scale glass powder inclusions [3]. Dine Elhannani et al. extended the Eshelby approach to examine the behavior of various mineral nano-inclusions in beam elements [4]. Similarly, Kecir et al. studied the bending behavior of slabs reinforced with iron oxide nanoparticles, where the rigidity of the biphasic composite system was determined using Eshelby's formulation [5]. Given the abundance of natural reinforcement sources, bio-based materials have

attracted considerable scientific attention. A comprehensive review by Haidee Yulady Jaramillo et al. reported more than 1,500 published studies on the incorporation of biomaterials into concrete [6]. Schmidt et al. investigated self-compacting and high-performance concretes produced using rice husk ash, cassava starch, lignosulfonate, and sisal fibers, demonstrating improved durability characteristics [7]. Kawaai et al. highlighted the effectiveness of bio-based additives such as alginate and *Bacillus subtilis* in crack-sealing and repair mortars, noting reduced capillarity and enhanced reliability [8]. Farhan Fatahillah et al. incorporated fly ash and eggshell powder into concrete mixtures, observing performance improvements in calcined concrete specimens [9]. Experimental investigations have further confirmed the mechanical benefits of bio-derived materials. Oussama Zaid et al. showed that adding 5% to 10% eggshell powder and nano-silica enhances the strength of ultra-high-performance fiber-reinforced concrete, although higher percentages reduce performance [10]. Shcherban et al. identified 10% eggshell powder as the optimal proportion for minimizing deformation under axial compression and tension [11]. Javed Ahmad Bhat et al. demonstrated that animal bones can serve as aggregates in lightweight concrete, achieving compressive strengths of approximately 20 MPa [12]. Konitufe Claudius et al. reported a 5% improvement in mechanical properties when using pulverized animal bones and bone ash [13]. Other researchers confirmed that fish bones, fish scales, and related biomaterials enhance strength while maintaining compliance with construction standards and reducing environmental impact, including CO_2 emissions [14–18]. Since concrete structures are continuously exposed to dynamic actions such as wind loads, seismic activity, and ocean waves, analyzing their vibration behavior is essential. Ding Hao-jiang et al. developed a mathematical formulation to predict static bending and free vibration of layered isotropic plates, identifying two independent vibration classes [19]. Alfano and Pagnotta determined Poisson's ratio and dynamic Young's modulus from natural vibration frequencies of thin rectangular plates [20]. Turan and co-authors extensively employed Higher-Order Shear Deformation Theory (HSDT) to analyze vibration and buckling in shells and laminated plates, incorporating orthotropic behavior and porosity effects [21–26]. Additional studies investigated seismic structural dynamics, elastic foundations, and beam vibrations using analytical methods such as KP-Ritz, Stodola–Vianello iteration, and Euler–Bernoulli formulations [27–32]. Bio-ceramic materials derived from natural

waste are particularly rich in nano-calcium carbonate. For example, eggshells contain approximately 98% Ca-CO_3, making them a highly valuable resource for sustainable material development [33–35]. Abdulkareem Adil Al-Ani, Hilal et al investigate the dynamic behavior of concrete slabs reinforced with silica nanoparticles (NS), which improve the microstructure by accelerating hydration and reducing porosity. Using a refined quasi-3D plate theory combined with Eshelby's homogenization model, they analyze slabs resting on elastic and viscoelastic foundations. Their results show that adding 30 wt% NS increases Young's modulus by about 26% and raises the fundamental natural frequency by up to 18%, with foundation parameters significantly affecting the vibrational response [56]. Benfrid et al. study the use of waste glass nan-opowder (GNP) as a sustainable additive to improve the thermal and mechanical performance of eco-concrete for wall applications. Using homogenization models (Maxwell–Eucken for thermal conductivity and Luo for elastic properties), they evaluate the elasto-thermo-mechanical behavior of nano-reinforced concrete. Results show that 30% GNP increases thermal conductivity by ~15% and thermal resistance by 25%, while reducing thermal expansion and the U-value by about 30% and 25%, confirming its potential for energy-efficient and eco-friendly structural walls [57]. Zouaoui et al. investigate the effect of incorporating nanosized Fe_2O_3 particles as fillers in concrete slabs and their influence on thermo-mechanical behavior. The study uses a refined trigonometric shear deformation theory (RTSDT) with stochastic Eshelby homogenization to determine thermoelastic properties, considering mechanical loads, temperature fields, and a three-parameter viscoelastic foundation (Winkler, Pasternak, damping). Results show that Fe_2O_3 nanoparticles improve mechanical resistance but may reduce thermal performance, while the viscoelastic foundation helps mitigate these negative thermal effects and enhances overall slab behavior [58]. Melati Lakhder et al. analytically investigates the flexural behavior of nanocomposite plates reinforced with a steel–nano-tungsten alloy, known for high thermal and corrosion resistance. The study applies a refined plate theory (RPT) with a sinusoidal shape function and only four unknowns, capturing both normal and shear deformations. Using the Mori–Tanaka homogenization model to estimate effective elastic properties, results are validated with existing solutions and show that reinforcement and geometric parameters strongly influence plate stresses and deflections [59]. Chatbi et al. study the static behavior of simply supported concrete beams reinforced with different

types of clay nano-platelets (NCs) using a quasi-3D beam theory. The effective elastic properties are obtained through Eshelby's homogenization model, while soil–structure interaction is modeled with a Winkler–Pasternak elastic foundation. Using the principle of virtual work and Navier-based analytical solutions, the results show that nanoplatelet type, volume fraction, geometry, and foundation parameters significantly influence beam deflection and mechanical resistance, confirming the efficiency of clay nano-platelets in strengthening concrete beams [60]. Ahmed Bassoud Ahmed et al. use density functional theory (DFT) to investigate the structural, electronic, and elastic properties of hydride perovskites $XCaH_3$ (X = Na, K, Rb, Cs). Energy–volume optimization confirms their stability in the cubic perovskite phase, while band structure analysis shows semiconducting behavior with direct band gaps (≈2.51–3.35 eV). Elastic constants satisfy Born stability criteria, and calculated moduli indicate these materials are mechanically stable, ductile, and potentially suitable for future energy applications [61]. Hamza Bouchehit et al. investigate the vibration behavior and soil–structure interaction of steel storage tanks. Their study analyzes the dynamic response of tanks considering the influence of supporting soil conditions on stability and structural performance. Results highlight the significant role of soil flexibility in modifying natural frequencies and vibration characteristics of steel tanks [62]. Boukhari Ahmed et al. study the bending behavior of concrete beams reinforced with granite waste powder using an improved beam theory combined with the virtual work principle and Navier's analytical solution. The effective mechanical properties of the granite–concrete composite are estimated using the Mori–Tanaka homogenization model. Results show that increasing the granite powder volume fraction enhances elastic and shear properties, leading to reduced beam deflection and transverse displacement, while also offering economic and environmental benefits through waste recycling and reduced emissions [63]. Abdelkader Yerkrou et al. study the mechanical and thermal buckling behavior of concrete panels incorporating glass waste and red brick waste as sustainable additives. Using the Mori–Tanaka homogenization model, they determine the thermo-mechanical properties of the biphasic mixture and evaluate critical buckling load and critical buckling temperature through FSDT (with a 5/6 correction factor). Results show that waste addition improves mechanical properties but generally reduces thermal performance, significantly affecting buckling behavior, with brick waste giving better thermal buckling resistance than glass

waste [64]. Abdelmoutalib Benfrid et al. investigate the thermal buckling instability of polymer panels used in water and oil reservoirs reinforced with short glass particulates. Several studies have investigated the thermal, mechanical, and dynamic behavior of advanced cementitious, composite, and structural materials. Abdelmoutalib et al. examined the thermal instability of a polymer panel reinforced with glass particles in order to evaluate its response under thermal effects [65] Benfrid proposed a biphasic homogenization approach for predicting the thermal and mechanical properties of eco-concretes [66]. Belmahi et al. analyzed the influence of acidic and alkaline environments on the mechanical properties of cement mortars [67]. Benfrid investigated the elastomechanical properties of concrete modified with aluminum nano-inclusions [69]. Khetir et al. studied the contribution of bio-sourced nanocomposites to the mechanical performance of a simply supported lightweight concrete beam [70]. Chatbi et al. demonstrated the effect of nano-clay platelets on improving the bending performance of concrete beams resting on elastic foundations [71]. Harrat et al. modeled the dynamic response of concrete beams modified with clay nanoparticles and supported by two-parameter elastic foundations [72]. Zahafi et al. proposed a lumped-parameter model for analyzing the vertical vibrations of surface circular foundations resting on nonhomogeneous soil [73]. Bencharif et al. presented a time-domain implementation of soil–structure interaction techniques using frequency-dependent impedance functions [74]. Chatbi et al. investigated the incorporation of nano-clay platelets to enhance the flexural behavior of concrete beams on elastic foundations [75]. Chatbi et al. studied the free vibration of composite beams reinforced with randomly aligned carbon nanotubes and resting on an elastic foundation [76]. Bencharif et al. developed a hybrid BEM-TLM-PML method to calculate the dynamic impedance functions of a rigid strip footing resting on nearly saturated poroelastic soil [77]. Tebbouche et al. characterized the El Kherba landslide triggered by the August 7, 2020 Mila earthquake using post-event field observations and ambient noise analysis [78]. Benfrid carried out a theoretical comparative study of homogenization models to estimate the effective properties of environmental concretes [79]. Sid Ahmed et al. analyzed the mechanical properties of thermally treated plastic-pozzolanic modified mortars [80]. Sid Ahmed et al. developed eco-friendly composite mortars for sustainable construction by assessing their rheological, thermo-mechanical, durability, and environmental performance [81]. Turan

and Benfrid investigated the free vibration of higher-order shear deformable porous orthotropic beams [82]. Benfrid analyzed the free vibration of a building raft foundation reinforced with short steel fibers [83]. Benfrid and Turan studied heat transfer in eco-friendly concrete panels containing low concentrations of recycled cardboard [84]. Abdelmoutalib et al. also examined the thermal instability of a polymer panel reinforced with glass particles [85]. Mladenov and Doicheva presented illustrative applications related to the behavior of simply supported beams [86]. Mladenov and Doicheva analyzed the flexural-torsional buckling of an eccentrically supported beam [87]. Doicheva proposed an exact solution for a beam resting on off-center elastic supports [88]. Doicheva investigated the critical and post-critical behavior of a T-shaped frame [89]. Mladenov and Doicheva analyzed the critical and post-critical behavior of a water tower with a conical tank [90]. Mladenov and Doicheva studied the flexural-torsional buckling of a beam supported by elastic rotational springs [91]. Doicheva and Mladenov examined dynamic characteristics used in the analysis of building structures [92]. Doicheva analyzed the shear force in interior beam–column joints subjected to two symmetrical transverse forces applied to the beam [93]. Doicheva studied the variation of shear force in reinforced concrete internal beam–column connections when the transverse load occupies different positions along the beam [94]. Doicheva investigated the effect of crack initiation and growth in a cantilever beam on the shear force of an internal beam–column joint [95]. Doicheva examined the influence of two symmetrical uniformly distributed loads placed at different positions on the shear force of an internal beam–column connection [96]. Doicheva studied the horizontal shear force in reinforced concrete internal beam–column connections during crack initiation and propagation caused by a linearly distributed load on a cantilever beam [97]. The study on plaster beams proposed a new approach for investigating the bending behavior of elements reinforced with short nano-bio-fibres using the Algerian DISS method [98]. Benfrid et al. investigated the thermal insulation performance of bio-based concrete made from apricot kernels [99]. Finally, Benfrid et al. analyzed the enhancement of the thermal efficiency of bio-concrete reinforced with wheat straw nanofibers for energy-efficient buildings [100].

The study aims to evaluate how adding 10% and 20% glass particulates, while improving mechanical strength, may negatively affect thermal buckling resistance. A

calculation script is developed to predict the thermal buckling behavior of these reinforced polymer panels and assess their structural reliability under thermal loading [65]. The present work is structured into two main parts. The first part focuses on the homogenization of concrete reinforced with 5% and 10% nano-calcium carbonate using the Hashin–Shtrikman model [36], which provides reliable bounds for estimating the effective properties of biphasic composite materials. Previous research has validated the accuracy of this model in predicting elastic and thermal properties of concrete composites [37–40]. Additional studies have also addressed waste recycling, pozzolanic additives, and innovative sustainable concrete formulations [51–55].The second part investigates the free vibration behavior of slabs made from conventional concrete and compares them with raft foundations reinforced with 5% and 10% nano-calcium carbonate. The developed model is validated against established theoretical formulations. The obtained results enable a detailed analysis of natural frequencies and vibration modes, providing valuable insight for future seismic evaluations. Since raft foundations are subjected to dynamic excitations and vibrate freely under environmental and seismic loads, special attention is given to the vibration response of slabs reinforced with bio-based nanomaterials, aiming to better understand their structural performance under realistic dynamic conditions.

2 HOMOGENIZATION HASHIN-SHTRIKMAN MODEL

The Hashin–Shtrikman model [36] is widely employed in scientific research for estimating the effective properties of composite materials. BENFRID et al. applied this model to homogenize concrete reinforced with glass nanoparticles [41]. Yiguo Zhang et al. used the Hashin–Shtrikman formulation to investigate the interfacial transition zone (ITZ) in concrete, as well as its influence on durability and mechanical resistance [42]. Raimondo Luciano J. and R. Willis combined the Hashin–Shtrikman approach with the finite element method to examine the impact of non-local interactions in concrete structures [43]. Fatima Aouissi et al. compared biphasic and triphasic homogenization models to predict the elastic modulus of concrete, relying on the Hashin–Shtrikman framework to model ITZ interactions [44]. Chunxiang Shi et al. also used this model to evaluate the effective elastic properties of concrete composites [45].

In the present section, the homogenization process is assumed to be biphasic and ideal. The interaction stresses between the matrix and the reinforcement are neglected, and the resulting composite material is considered homogeneous and isotropic after homogenization. The concrete is taken as the matrix phase, while bio-sourced nano-calcium carbonate is considered the reinforcement phase, introduced with volume fractions of 10% and 20%.

The two bounds of the compressibility modulus:

$$\begin{aligned} K^{*-} &= K_M + \frac{V_R}{(K_R - K_M)^{-1} + 3(1-V_R)(3K_M + 4G_M)^{-1}}; \\ K^{*+} &= K_R + \frac{V_M}{(K_M - K_R)^{-1} + 3V_R(3K_R + 4G_R)^{-1}}; \\ K^{*-} &\le K^* \le K^{*+} \end{aligned} \qquad (1)$$

The two bounds of the shear modulus:

$$\begin{aligned} G^{*-} &= G_M + \frac{V_R}{(G_R - G_M)^{-1} + 6(1-V_R)(K_M + 2G_M)(5G_M(3K_M + 4G_M))^{-1}}; \\ G^{*+} &= G_R + \frac{V_M}{(G_M - G_R)^{-1} + 6V_R(K_R + 2G_R)(5G_R(3K_R + 4G_R))^{-1}}; \\ G^{*-} &\le G^* \le G^{*+} \end{aligned} \qquad (2)$$

The two bounds of the elasticity modulus:

$$E^{*+} = \frac{9K^+G^+}{3K^+ + G^+}; E^{*-} = \frac{9K^-G^-}{3K^- + G^-}; E^{*-} \le E^* \le E^{*+} \qquad (3)$$

The Poisson's ratio:

$$\nu^{*-}=\frac{3K^{-}-2G^{-}}{6K^{-}+2G^{-}};\nu^{*+}=\frac{3K^{+}-2G^{+}}{6K^{+}+2G^{+}};\nu^{*-}\le\nu^{*}\le\nu^{*+} \qquad (4)$$

Noted that:

- K^{*+}: Superior homogeneous compressibility modulus.
- K^{*-}: Lower homogeneous compressibility modulus.
- K^{*}: Average homogeneous compressibility modulus.
- K_M: Compressive modulus of the matrix (concrete).
- K_R: Compressive modulus of the reinforcement (nano-calcium carbonate).
- G^{+}: Superior homogeneous Shear modulus.
- G^{-}: Lower homogeneous Shear modulus.
- G^{*}: Average homogeneous Shear modulus.
- G_M: Shear modulus of the matrix (concrete).
- G_R: Shear modulus of the reinforcement (nano-calcium carbonate).
- E^{*+}: Superior homogeneous Elastic's modulus.
- E^{*-}: Lower homogeneous Elastic's modulus.
- E^{*}: Average homogeneous Elastic's modulus.
- E_M: Elastic's modulus of the matrix (concrete).
- E_R: Elastic's modulus of the reinforcement (nano-calcium carbonate).
- ν^{*+}: Superior homogeneous Poisson's ratio.
- ν^{*-}: Lower homogeneous Poisson's ratio.
- ν^{*}: Average homogeneous Poisson's ratio.
- ν_M: Poisson's ratio of the matrix (concrete).
- ν_R: Poisson's ratio of the reinforcement (nano-calcium carbonate).
- V_M: Volume fraction of the matrix (concrete).
- V_R: Volume fraction of the reinforcement (nano-calcium carbonate).

When:

$$K_M = \frac{E_M}{3(1-2\nu_M)}; K_R = \frac{E_R}{3(1-2\nu_R)};$$

$$G_M = \frac{E_M}{2(1+\nu_M)}; G_R = \frac{E_R}{2(1+\nu_R)}; \quad (5)$$

For Density

$$\rho^* = V_R\rho_R + V_M\rho_M$$

In which:

$$V_{Matrix+Reinforcement} = V_M + V_R = 1 \quad (6)$$

3 PROGRAMMING THE VIBRATION BEHAVIOR

In this section, the slab is simply supported, composed of concrete reinforced with nano-calcium carbonate, as shown in Figure 1.

Figure 1

A simply supported concrete slab, reinforced with different volume fraction of nano-calcium carbonate

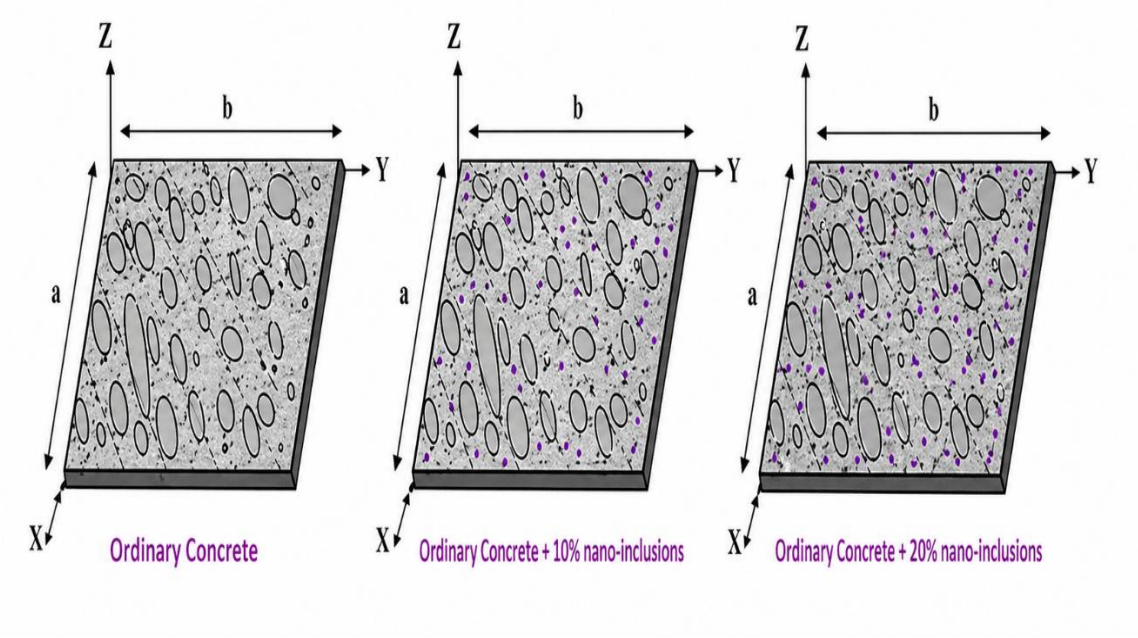

The displacements are defined:

$$U(x,y,z) = u_0(x,y) - z\frac{\partial w_b(x,y)}{\partial x} - f(z)\frac{\partial w_s(x,y)}{\partial x} \quad (7)$$

$$V(x,y,z) = v_0(x,y) - z\frac{\partial w_b(x,y)}{\partial y} - f(z)\frac{\partial w_s(x,y)}{\partial y} \quad (8)$$

$$W(x,y,z) = w_b(x,y) + w_s(x,y) \quad (9)$$

The displacements in the x and y directions at a point on the mid-plane of the slab are denoted as (u_o, v_o), while (w_b, w_s) represent the buckling and shear components, respectively, of the transverse displacement $f(z)$. Same for [41]:

$$\begin{aligned} &f(z) = z; g(z) = \frac{\partial f(z)}{\partial z}\ ; \kappa_s = \frac{5}{6} && \text{FSDT} \\ &f(z) = z\left(1 - \frac{4}{3}\frac{z^2}{h^2}\right); g(z) = \frac{\partial f(z)}{\partial z}\ ; \kappa_s = 1 && \text{HSDT} \end{aligned} \quad (10)$$

The constitutive stress-strain relationships:

$$\begin{Bmatrix} \sigma_x \\ \sigma_y \\ \tau_{xy} \\ \tau_{xz} \\ \tau_{yz} \end{Bmatrix} = \begin{bmatrix} Q_{11} & Q_{12} & 0 & 0 & 0 \\ Q_{21} & Q_{22} & 0 & 0 & 0 \\ 0 & 0 & Q_{33} & 0 & 0 \\ 0 & 0 & 0 & Q_{44} & 0 \\ 0 & 0 & 0 & 0 & Q_{55} \end{bmatrix} \begin{Bmatrix} \varepsilon_x \\ \varepsilon_y \\ 2\gamma_{xy} \\ 2\gamma_{xz} \\ 2\gamma_{yz} \end{Bmatrix} \quad (11)$$

when:

$$Q_{11} = Q_{22} = \frac{(1-\nu^*)E^*}{(1+\nu^*)(1-2\nu^*)}; Q_{12} = Q_{21} = \frac{\nu^* E^*}{(1+\nu^*)(1-2\nu^*)} \quad (12)$$

$$Q_{33} = Q_{44} = Q_{55} = G^* = \frac{E^*}{2(1+\nu^*)} \qquad (13)$$

The components of the different deformations and distortions:

$$\varepsilon_x = \frac{\partial U}{\partial x}; \varepsilon_y = \frac{\partial V}{\partial y}; 2\gamma_{xy} = \frac{\partial U}{\partial x} + \frac{\partial V}{\partial y}; 2\gamma_{xz} = \frac{\partial U}{\partial z} + \frac{\partial W}{\partial x}; 2\gamma_{yz} = \frac{\partial V}{\partial z} + \frac{\partial W}{\partial y} \qquad (14)$$

The principle of virtual work is applied to determine the mechanical bending response of the slab:

$$\int_0^t (\delta U + \delta V) dt = 0 \qquad (15)$$

δU is given by the following expression and represents the virtual variations of the internal strain energy within this slab:

$$\delta U = \int_0^A \int_{\frac{-h}{2}}^{\frac{h}{2}} (\sigma_x \delta\varepsilon_x + \sigma_y \delta\varepsilon_y + \tau_{xy}\delta\gamma_{xy} + \tau_{yz}\delta\gamma_{yz} + \tau_{xz}\delta\gamma_{xz}) dA dz \qquad (16)$$

Introducing equations (14) to (16) into the previous equation (17), they yield:

$$\delta U = \int_A (N_x \frac{\partial \delta u_0}{\partial x} - M^b{}_x \frac{\partial^2 \delta w_b}{\partial^2 x} + M^s{}_x \frac{\partial^2 \delta w_s}{\partial^2 x} + N_y \frac{\partial \delta v_0}{\partial y} - M^b{}_x \frac{\partial^2 \delta w_b}{\partial^2 y} + M^s{}_x \frac{\partial^2 \delta w_s}{\partial^2 y}$$
$$+ N_{xy}(\frac{\partial \delta u_0}{\partial y} + \frac{\partial \delta v_0}{\partial x}) + 2M^b{}_x \frac{\partial^2 \delta w_b}{\partial x \partial y} + 2M^s{}_x \frac{\partial^2 \delta w_s}{\partial x \partial y} + Q_{yz} \frac{\partial \delta w_s}{\partial y} + Q_{xz} \frac{\partial \delta w_s}{\partial x} - I_{xy} \frac{\partial \delta w_s}{\partial y} - I_{xy} \frac{\partial \delta w_b}{\partial y} \qquad (17)$$

The resultants of stresses and moments (*N, M_b, M_s, Q (mechanical case) :*

$$N_{ij} = b\int_{\frac{-h}{2}}^{\frac{-h}{2}} \sigma_{ij} dz \; ; M^{b}_{ij} = b\int_{\frac{-h}{2}}^{\frac{-h}{2}} z\sigma_{ij} dz \; ; M^{s}_{ij} = b\int_{\frac{-h}{2}}^{\frac{-h}{2}} f(z)\sigma_{ij} dz \; ; Q_{ij} = b\int_{\frac{-h}{2}}^{\frac{-h}{2}} g(z)\kappa_s \sigma_{ij} dz \tag{18}$$

Note that *i* or j correspond to *x* or *y*.

δV represents the virtual external energy induced by the external mechanical loads *(N (mechanical loads) and T (Thermal Loads))* and is defined as:

$$\delta V = -\int_A \int_{\frac{-h}{2}}^{\frac{h}{2}} N\delta W dA dz; \delta V = -\int_A \int_{\frac{-h}{2}}^{\frac{h}{2}} T\delta W dA dz \tag{19}$$

By substituting equation (19 and 18) with equation (17), which depends on equation (20), and performing integration by parts while considering the coefficients of δu_0 , δv_0 , δw_b and δw_s, the resulting equations of motion are derived as follows:

$$\delta u_0 : \frac{\partial N_x}{\partial x} + \frac{\partial N_{xy}}{\partial y} = I_0 X'' \tag{20}$$

$$\delta v_0 : \frac{\partial N_y}{\partial y} + \frac{\partial N_{xy}}{\partial x} = I_0 Y'' \tag{21}$$

$$\delta w_b : \frac{\partial^2 M^{b}_{x}}{\partial x^2} - 2\frac{\partial^2 M^{b}_{xy}}{\partial x \partial y} + \frac{\partial^2 M^{b}_{y}}{\partial y^2} + N = I_0(Z_s'' + Z_b'') + I_2 \frac{\partial^2 w_s}{\partial x^2} + I_2 \frac{\partial^2 w_b}{\partial x^2} \tag{22}$$

$$\delta w_s : \frac{\partial^2 M^{s}_{x}}{\partial x^2} - 2\frac{\partial^2 M^{s}_{xy}}{\partial x \partial y} + \frac{\partial^2 M^{s}_{y}}{\partial y^2} + \frac{\partial Q_{xz}}{\partial x} + \frac{\partial Q_{yz}}{\partial y} + N = I_0(Z_s'' + Z_b'') + I_2 \frac{\partial^2 w_s}{\partial x^2} + I_2 \frac{\partial^2 w_b}{\partial x^2} \tag{23}$$

Given the simply supported rectangular panel, shown in Figure 1, with a length "*a*", a width "*b*", and a total thickness "*h*", the boundary conditions are defined as follows:

$$\begin{aligned} &x = 0; x = a; v_0 = w_b = w_s = N_x = M_x{}^b = M_x{}^s = 0 \\ &y = 0; x = b; u_0 = w_b = w_s = N_y = M_y{}^b = M_y{}^s = 0 \end{aligned} \quad (24)$$

The free vibration

$$[K] - \omega^2[m]\{\Delta\} = 0 \quad (25)$$

Using Navier's solution for the simply supported plate case, the admissible displacement functions will be expressed in the following manner to satisfy the boundary conditions outlined in the equation (35).

$$u(x,y) = \sum_{m=1}^{\infty}\sum_{n=1}^{\infty} X_{mn}\cos(\xi x)\sin(\varsigma x)e^{i\omega t} \quad (26)$$

$$v(x,y) = \sum_{m=1}^{\infty}\sum_{n=1}^{\infty} Y_{mn}\cos(\xi x)\sin(\varsigma x)e^{i\omega t} \quad (27)$$

$$w_b(x,y) = \sum_{m=1}^{\infty}\sum_{n=1}^{\infty} Z_{bmn}\sin(\xi x)\sin(\varsigma x)e^{i\omega t} \quad (28)$$

$$w_s(x,y) = \sum_{m=1}^{\infty}\sum_{n=1}^{\infty} Z_{smn}\sin(\xi x)\sin(\varsigma x)e^{i\omega t} \quad (29)$$

(X_{mn}, Y_{mn}, Z_{bmn}, Z_{smn}) are the arbitrary parameters to be determined.

Where:

$$\xi = \frac{m\pi}{a}; \varsigma = \frac{n\pi}{b} \quad (30)$$

Finally, to derive the analytical solutions, the results of the substitution can be presented in the following matrix form:

$$\left(\begin{bmatrix} K_{11} & K_{12} & K_{13} & K_{14} \\ K_{12} & K_{22} & K_{23} & K_{24} \\ K_{13} & K_{23} & K_{33} & K_{34} \\ K_{14} & K_{24} & K_{34} & K_{44} \end{bmatrix} - \omega^2 \begin{bmatrix} m_{11} & 0 & 0 & 0 \\ 0 & m_{22} & 0 & 0 \\ 0 & 0 & m_{33} & m_{44} \\ 0 & 0 & m_{34} & m_{44} \end{bmatrix}\right) \begin{Bmatrix} X_{mn} \\ Y_{mn} \\ Z_{bmn} \\ Z_{smn} \end{Bmatrix} = \begin{Bmatrix} 0 \\ 0 \\ 0 \\ 0 \end{Bmatrix} \quad (31)$$

When:

$$\begin{aligned} &I_0, I_1, I_2 = \iiint (1, z, z^2)\rho dz; \\ &m_{11} = m_{22} = m_{34} = I_0; \\ &m_{33} = I_0 + I_1(\zeta^2 + \varsigma^2); \\ &m_{44} = I_0 + I_2(\zeta^2 + \varsigma^2); \end{aligned} \quad (32)$$

After resolve N in mechanical Loads (Dimensionless parameter):

$$\varpi : solve([K] - \omega^2[m]\{\Delta\} = 0) \quad (33)$$

Not that we have three frutescence's:

$$\varpi_1 = \omega * h\sqrt{\frac{\rho_m}{G_m}} \quad (34)$$

In which:

$$\begin{aligned} &K_{11} = -A_{11}\xi^2 - A_{33}\varsigma^2; K_{12} = -\xi\varsigma(A_{33} + A_{12}); K_{13} = B_{11}\xi^3 + (2B_{66} + B_{12})\xi\varsigma^2; \\ &K_{14} = B^s{}_{11}\xi^3 + (2B^s{}_{66} + B^s{}_{12})\xi\varsigma^2; K_{22} = -A_{11}\xi^2 + A_{33}\varsigma^2; K_{23} = -B_{22}\varsigma^3 + (2B_{33} + B_{12})\varsigma\xi^2; \end{aligned} \quad (35)$$

$$\begin{aligned} &K_{24} = -B^s{}_{22}\varsigma^3 + (2B^s{}_{33} + B^s{}_{12})\varsigma\xi^2; K_{33} = -D_{11}\xi^4 + 2(D_{12} + 2D_{33})(\varsigma\xi)^2 + D_{22}\varsigma^2; \\ &K_{34} = -D^s{}_{11}\xi^4 + 2(D^s{}_{12} + 2D^s{}_{33})(\varsigma\xi)^2 + D^s{}_{22}\varsigma^2; N_{33} = \varsigma^2 + \lambda\xi^2 \\ &K_{44} = -A^{s*}{}_{11}\xi^4 - 2(A^{s*}{}_{12} + 2A^{s*}{}_{33})(\varsigma\xi)^2 + A^{s*}{}_{22}\varsigma^2 + A^{c*}{}_{55}\xi^2 + A^{c*}{}_{44}\varsigma^2; \end{aligned} \quad (36)$$

when:

$$A_{ij} = b\int_{\frac{-h}{2}}^{\frac{h}{2}} Q_{ij}dz; B_{ij} = b\int_{\frac{-h}{2}}^{\frac{h}{2}} Q_{ij}zdz; D_{ij} = b\int_{\frac{-h}{2}}^{\frac{h}{2}} Q_{ij}z^2dz; A^s{}_{ij} = b\int_{\frac{-h}{2}}^{\frac{h}{2}} Q_{ij}f(z)dz; B^S{}_{ij} = b\int_{\frac{-h}{2}}^{\frac{h}{2}} Q_{ij}zf(z)dz; \quad (37)$$

$$A^{s*}{}_{ij} = b\int_{\frac{-h}{2}}^{\frac{h}{2}} Q_{ij}z\kappa_s f^2(z)dz; A^{c*}{}_{ij} = b\int_{\frac{-h}{2}}^{\frac{h}{2}} Q_{ij}\kappa_s g(z)dz; \quad (38)$$

4 RESULTS AND DISCUSSION

Table 1 summarizes the mechanical properties of the concrete matrix and the nano-calcium carbonate nanoparticles used as reinforcement in this study. Table 2 presents the properties of ordinary concrete and nano-calcium carbonate-reinforced concrete.

Table 1

The mechanical properties of concrete as the matrix and nano-Nano-calcium Carbonate as the reinforcement [47] an [48].

Properties	*Matrix (Concrete)*	*Concrete [47]*	*Reinforced (nano-calcium carbonate)*	*nano-Nano-calcium Carbonate [48]*
Elastic modulus	E_M *(GPa)*	*20*	E_R *(GPa)*	*68.7*
Poisson's ratio	$\boldsymbol{\nu}_M$	*0.3*	$\boldsymbol{\nu}_R$	*0.329*
Shear modulus	G_M *(GPa)*	*7.79*	G_R *(GPa)*	*25.82*
Bulk modulus	K_M *(GPa)*	*16.67*	K_R *(GPa)*	*67.08*
Density	$\rho_M(Kg/m^3)$	*2500*	$\rho_R(Kg/m^3)$	*2620*

Table 2

The effective mechanical properties of concrete reinforced with 10% and 20% nano-calcium carbonate, compared to ordinary concrete.

Properties	*Elastic modulus*	Poisson's ratio	Shear modulus	Bulk modulus	Density
Symbols and Units	*E**	$\boldsymbol{\nu}^*$	*G**	K^*	ρ^*

	(GPa)		*(GPa)*	*(GPa)*	*(Kg/m³)*
V_w(0%)	*20*	*0.3*	*7.7*	*16.7*	*2520*
V_w(10%)	*22.9*	*0.31*	*8.8*	*19.2*	*2510*
V_w(20%)	*25.9*	*0.32*	*10.2*	*22.4*	*2515*

The incorporation of nano-$CaCO_3$ leads to a noticeable enhancement in Young's modulus, Poisson's ratio, compressibility, density, and shear modulus, indicating an overall improvement in the mechanical strength of the concrete, as reported in Table 2.

To validate and compare the proposed model, the material parameters were taken as =210 GPa, density ρ=7800 kg/m³, and Poisson's ratio ν=0.3\nu = 0.3ν=0.3, in accordance with the reference works presented in [49] and [50].

Table 3

Comparison between my obtained frequencies now by FSDT and HSDT with the review of Ghugal and Sayyad [49] for square plate (a=b) and rectangular plate when: $b=\sqrt{2}a$ and (a/h =10) isotope plate.

frequencies	ϖ_1	ϖ_1	ϖ_1	ϖ_1	ϖ_1	ϖ_1
Shape of plate	Square			Rectangular		
Modes/Methods	*Ghugal and Sayyad [49]*	*Present (FSDT)*	*Present (HSDT)*	*Ghugal and Sayyad [49]*	*Present (FSDT)*	*Present (HSDT)*
(1,1)	*0.0933*	*0.094*	*0.091*	*0.0705*	*0.071*	*0.068*
(1,2)	*0.2231*	*0.23*	*0.22*	*0.1393*	*0.14*	*0.13*
(1,3)	*0.4148*	*0.47*	*0.42*	*0.2438*	*0.25*	*0.24*

According to Table 3, the results obtained from both theories are in good agreement with those reported in the reference literature, which confirms the validity of the developed numerical implementation for frequency calculation. It is also observed that the Higher-Order Shear Deformation Theory (HSDT) provides more accurate predictions. Therefore, only the HSDT model will be used in the subsequent analysis.

Table 4 presents the variation of the natural frequencies for both square and rectangular slabs across different vibration modes, considering the two reinforcement volume fractions.

Table 4

Comparison between the frequencies of ordinary concrete and reinforced concrete for a square plate (a=b) and rectangular plate when: $b=\sqrt{2}a$ *and (a/h =10) isotope plate.*

frequencies	ϖ_1	ϖ_1	ϖ_1	ϖ_1	ϖ_1	ϖ_1
Shape of plate	Square			Rectangular		
Modes/Vf	*0%*	*10%*	*20%*	*0%*	*10%*	*20%*
(1,1)	*0.092*	*0.12*	*0.13*	*0.07*	*0.09*	*0.10*
(1,2)	*0.22*	*0.30*	*0.31*	*0.13*	*0.18*	*0.19*
(1,3)	*0.42*	*0.58*	*0.59*	*0.24*	*0.33*	*0.34*

The incorporation of nano-calcium carbonate into the concrete enhances its dynamic behavior, as evidenced by the increase in natural frequencies with higher nanoparticle volume fractions. This rise in frequency indicates an improvement in structural stiffness. The best performance is observed for reinforcement levels of 10% and 20%, as presented in Table 4.

Figure 2

The variation of length and thickness in the case of a square plate where (m = n = 1).

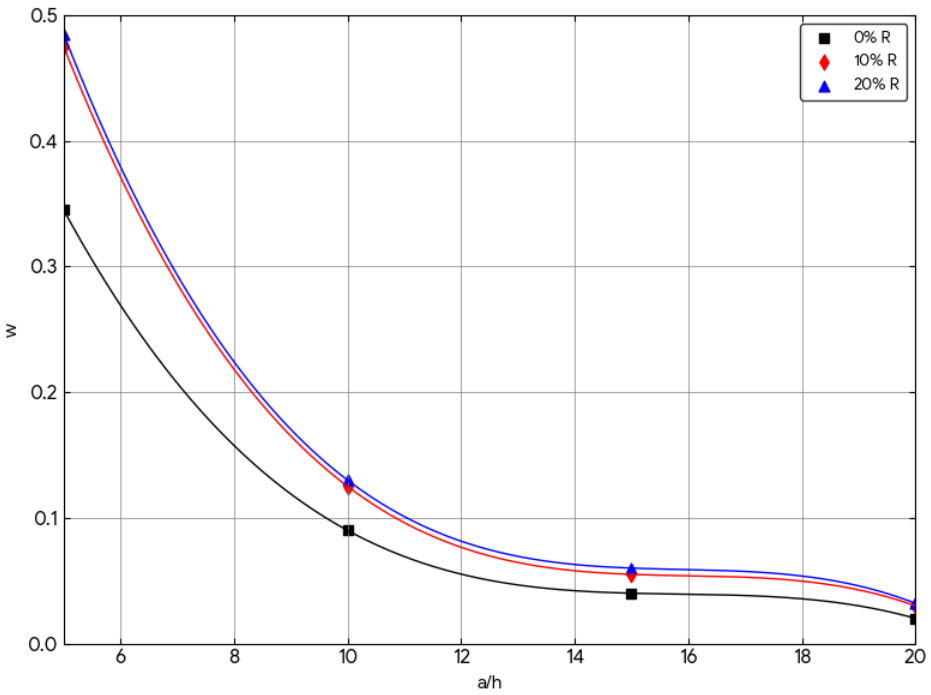

Figure 3

The variation of length and thickness in the case of a square plate where (m = n =2).

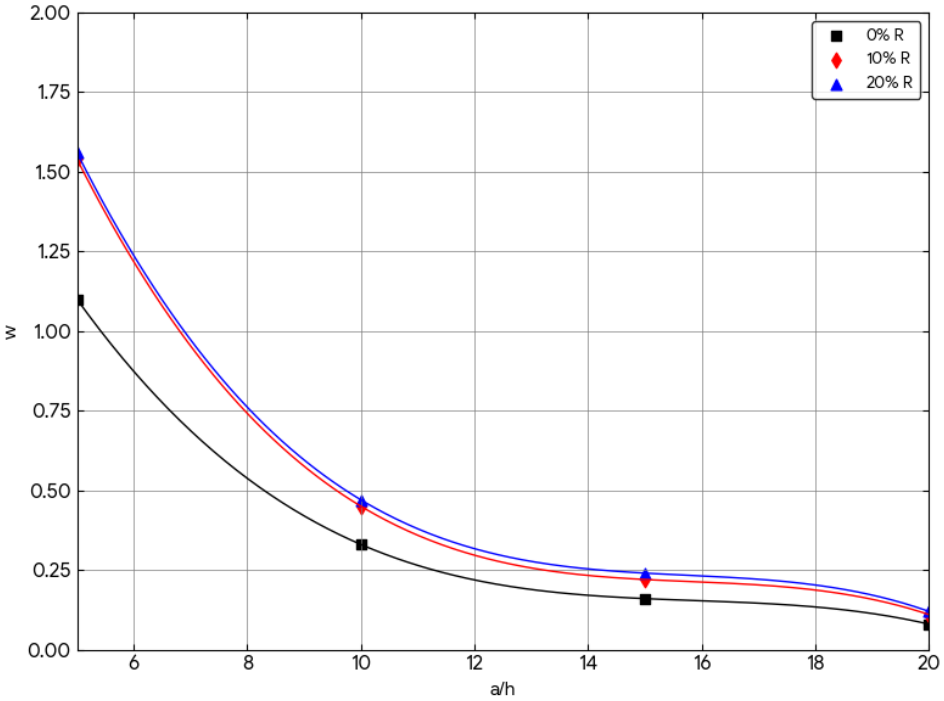

Figure 4

The variation of length and width with a=4h for the modes (m=n=1).

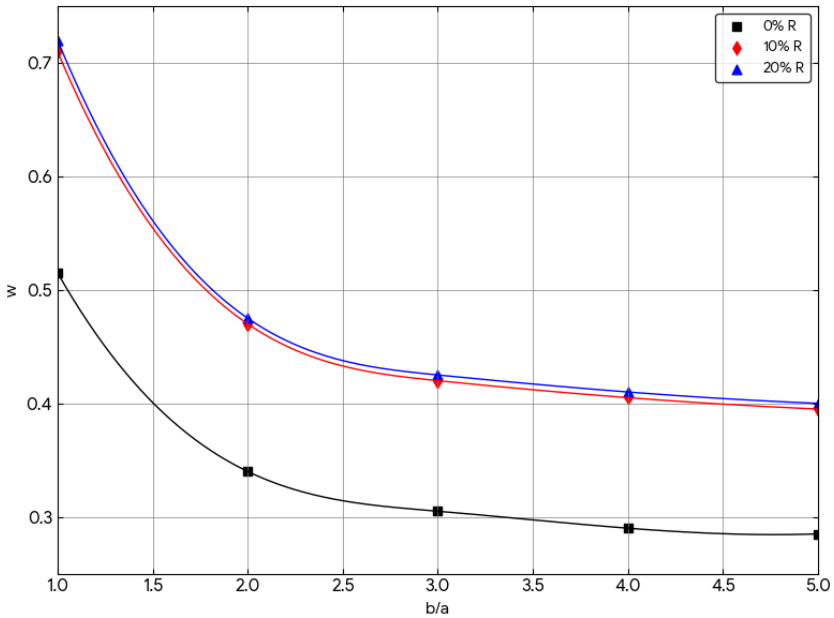

Figure 5

The variation of length and width with a=4h for the modes (m=n=2).

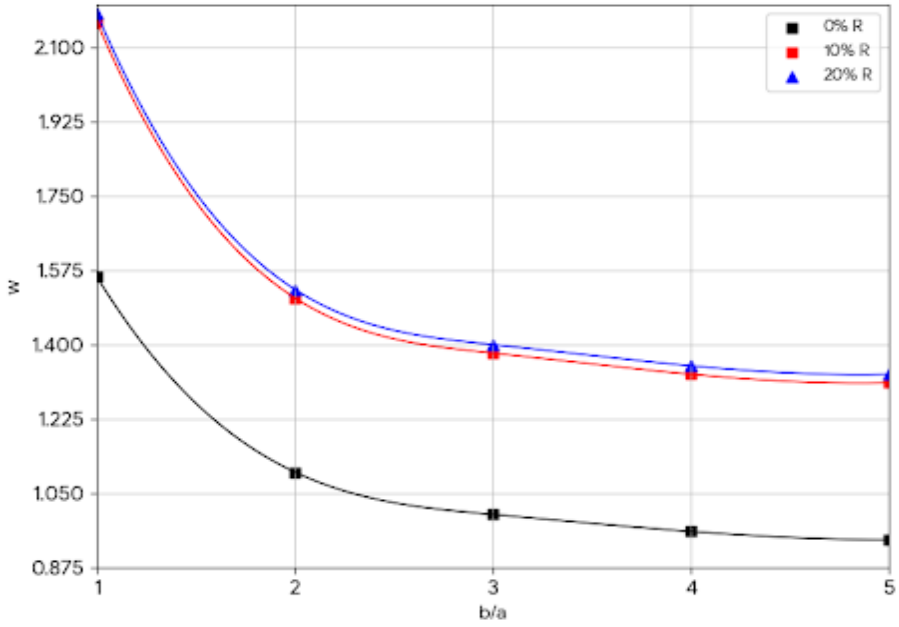

From Figure 2, it can be observed that the natural frequency decreases as the ratio a/h increases. It is also recalled that the optimal reinforcement content is 10% nano-$CaCO_3$. When the vibration mode changes, the frequency increases by nearly three times, as shown and compared in Figures 2 and 3.In Figures 5 and 6, the slab length is varied with respect to its width while keeping a/h=1. It is noted that increasing the ratio b/a leads to a reduction in the frequency. Concrete reinforced with 10% and 20% nano-$CaCO_3$ exhibits higher frequencies due to the increased stiffness of the raft foundation. In addition, the frequency in mode 1 remains lower than that in mode 2. However, the results indicate that an addition of only 10% nano-$CaCO_3$ is sufficient to achieve significant improvement. In the corner regions of Figures 3 and 4, the results become very close, since the slab becomes thicker.

5 CONCLUSION

The Hashin–Shtrikman model proves to be an effective tool for analyzing the

nanomechanical behavior of concrete, as it enables the estimation of equivalent mechanical properties at the nanoscale when nano-reinforcements are incorporated. The addition of nano-calcium carbonate progressively enhances the mechanical performance of concrete slabs, increasing the stiffness of the raft foundation and improving its resistance to vibrations. However, beyond a reinforcement level of 10%, the improvements become nearly marginal, making 10% the most suitable proportion from an economic perspective. Furthermore, the Higher-Order Shear Deformation Theory (HSDT) consistently provides more accurate results than classical theories for vibration analysis. The findings of this study demonstrate that concrete reinforced with nano-calcium carbonate exhibits greater durability and improved resistance to dynamic loading, while also contributing to environmental sustainability through the valorization of bio-based waste materials and the reduction of CO_2 emissions. This research opens promising perspectives in the field of nanotechnology applied to concrete, reduces reliance on extensive experimental campaigns, and provides a valuable reference for future investigations, particularly in vibration analysis and structural protection against seismic effects.

REFERENCES

[1] Harrat, Z. R., Amziane, S., Krour, B., & Bouiadjra, M. B. (2021). On the static behavior of nano SiO_2 based concrete beams resting on an elastic foundation. *Computers and Concrete*, *27*(6), 575–583. https://doi.org/10.12989/cac.2021.27.6.575

[2] Chatbi, M., Krour, B., Benatta, M. A., Harrat, Z. R., Amziane, S., & Bouiadjra, M. B. (2022). Bending analysis of nano-SiO_2 reinforced concrete raft foundation resting on elastic foundation. *Structural Engineering and Mechanics*, *84*(5), 685–697. https://doi.org/10.12989/sem.2022.84.5.685

[3] Benfrid, A., Benbakhti, A., Harrat, Z. R., Chatbi, M., Krour, B., & Bouiadjra, M. B. (2023). Thermomechanical analysis of glass powder based eco-concrete panels: Limitations and performance evaluation. *Periodica Polytechnica Civil Engineering*, *67*(4), 1284–1297. https://doi.org/10.3311/PPci.22781

[4] Elhennani, S. D., Harrat, Z. R., Chatbi, M., Belbachir, A., Krour, B., Işık, E., Harirchian, E., Bouremana, M., & Bouiadjra, M. B. (2023). Buckling and free vibration analyses of various nanoparticle reinforced concrete beams resting on multi-parameter elastic foundations. *Materials*, *16*(17), Article 5865. https://doi.org/10.3390/ma16175865

[5] Kecir, A., Chatbi, M., Harrat, Z. R., Bouiadjra, M. B., Bouremana, M., & Krour, B. (2024). Enhancing the mechanical performance of concrete raft foundation through the incorporation of nano-sized iron oxide particles (Fe_2O_3): Non-local bending analysis. *Periodica Polytechnica Civil Engineering*, *68*(3), 842–858. https://doi.org/10.3311/PPci.23016

[6] Jaramillo, H. Y., Vasco-Echeverri, O. H., Moreno-Pacheco, L. A., & García-León, R. A. (2023). Biomaterials in concrete for engineering applications: A bibliometric review. *Infrastructures*, *8*(11), Article 161. https://doi.org/10.3390/infrastructures8110161

[7] Schmidt, W., Msinjili, N. S., Pirskawetz, S., & Kühne, H. C. (2015). Efficiency of high performance concrete types incorporating bio-materials like rice husk ashes, cassava starch, lignosulfonate, and sisal fibres. *Academic Journal of Civil Engineering*, *33*(2), 208–214. https://doi.org/10.26168/icbbm2015.32

[8] Kawaai, K., Nishida, T., Saito, A., & Hayashi, T. (2022). Application de matériaux biosourcés aux méthodes de réparation des fissures et des patchs dans le béton. *Construction and Building Materials*, *340*, Article 127718. https://doi.org/10.1016/j.conbuildmat.2022.127718

[9] Fatahillah, F., & Sumarno, A. (2022). The effect of concrete mixture on usage fly ash and chicken egg shell powder as cement substitutions in concrete compressive strength. *Neutron*, *22*(1), 24–30. https://doi.org/10.29138/neutron.v22i01.173

[10] Zaid, O., Hashmi, S. R. Z., El Ouni, M. H., Martínez-García, R., De Prado-Gil, J., & Yousef, S. E. A. S. (2023). Experimental and analytical study of ultra-high-performance fiber-reinforced concrete modified with egg shell powder and nano-silica. *Journal of Materials Research and Technology*, *24*, 7162–7188. https://doi.org/10.1016/j.jmrt.2023.04.240

[11] Shcherban', E. M., Stel'makh, S. A., Beskopylny, A. N., Mailyan, L. R., Meskhi, B., Varavka, V., Beskopylny, N., & El'shaeva, D. (2022). Enhanced eco-friendly concrete nano-change with eggshell powder. *Applied Sciences*, *12*(13), Article 6606. https://doi.org/10.3390/app12136606

[12] Bhat, J., Qasab, R. A., & Dar, A. R. (2012). Machine crushed animal bones as partial replacement of coarse aggregates in lightweight concrete. *ARPN Journal of Engineering and Applied Sciences*, *7*(9), 1202–1207.

[13] Claudius, K., Baba, A. S., & Abubakar, A. (2023). Influence of pulverized animal bone and animal bone ash on the mechanical properties of normal strength concrete using response surface method. *Construction*, *3*(1), 63–74. https://doi.org/10.15282/construction.v3i1.9097

[14] Damayanti, S., Aulia, T. B., & Hayati, Y. (2020). The effect of fishbone fiber and rice husk ash additive on the mechanical properties of normal concrete. *IOP*

Conference Series: Materials Science and Engineering, *933*, Article 012036. https://doi.org/10.1088/1757-899X/933/1/012036

[15] Arain, F. A., Jatoi, M. A., Raza, M. S., Shaikh, F. A., Khowaja, F., & Rai, K. (2022). Preliminary investigation on properties of novel sustainable composite: Fish scales reinforced cement concrete. *Jurnal Kejuruteraan*, *34*(2), 309–315. https://doi.org/10.17576/jkukm-2022-34(2)-14

[16] Sulaiman, E. A., Alwash, J. J. H., Jasim, T. A., Al-Khafaji, Z., Falah, M., & Al-Edrus, S. S. A. O. (2025). Investigating the effect of applying fish scale powder in concrete as sustainable blending materials. *Review of Composite Materials and Applications*, *35*(3), 403–412. https://doi.org/10.18280/rcma.350302

[17] Higashino, T., Yanaka, A., Oyake, Y., Okazaki, S., Suenaga, Y., & Yoshida, H. (2025). Development of a porous concrete mixed with hydroxyapatite produced from fish bones. *GEOMATE Journal*, *28*(130), 112–122. https://geomatejournal.com/geomate/article/view/5068

[18] Yanaka, A., Yoshida, H., Okazaki, S., Oyake, Y., & Suenaga, Y. (2023). Recycling of fishery waste as planting base porous concrete aimed at achieving carbon neutrality. *GEOMATE Journal*, *24*(104), 85–92. https://geomatejournal.com/geomate/article/view/3845

[19] Ding, H., Chen, W., & Xu, R. (2001). On the bending, vibration and stability of laminated rectangular plates with transversely isotropic layers. *Applied Mathematics and Mechanics*, *22*(1), 17–24.

[20] Alfano, M., & Pagnotta, L. (2006). Determining the elastic constants of isotropic materials by modal vibration testing of rectangular thin plates. *Journal of Sound and Vibration*, *293*, 426–439. https://doi.org/10.1016/j.jsv.2005.10.021

[21] Turan, F. (2025). Natural frequencies of shear deformable porous orthotropic laminated doubly-curved shallow shells with non-uniformly distributed porosity using higher-order shear deformation theory. *Thin-Walled Structures*, *210*, Article 112951. https://doi.org/10.1016/j.tws.2025.112951

[22] Turan, F., Karadeniz, M., & Zeren, E. (2024). Free vibration and buckling behavior of porous orthotropic doubly-curved shallow shells subjected to non-uniform edge compression using higher-order shear deformation theory. *Thin-Walled Structures*, *205*(Part C), Article 112522. https://doi.org/10.1016/j.tws.2024.112522

[23] Turan, F. (2024). Free vibration response of multi-layered plates with trigonometrically distributed porosity based on the higher-order shear deformation theory. *Steel and Composite Structures*, *53*(1), 77–90. https://doi.org/10.12989/scs.2024.53.1.077

[24] Bahadir, F. C., & Turan, F. (2024). On the vibration responses of orthotropic laminated cylindrical panels with non-uniform porosity distributions using higher-

order shear deformation theory. *Mechanics Based Design of Structures and Machines*, *52*(12), 9975–10005. https://doi.org/10.1080/15397734.2024.2352585

[25] Turan, F. (2023). Vibration analysis of porous orthotropic cylindrical panels resting on elastic foundations based on shear deformation theory. *International Journal of Engineering and Applied Sciences*, *15*(3), 125–143. https://doi.org/10.24107/ijeas.1342775

[26] Turan, F. (2023). Natural frequencies of porous orthotropic two-layered plates within the shear deformation theory. *Challenge Journal of Structural Mechanics*. https://doi.org/10.20528/cjsmec.2023.01.001

[27] Doicheva, A., & Mladenov, K. (2005). On some dynamic characteristics in the analysis of building structures. In *Proceedings of the Scientific Conference with International Participation* (Vol. 1, pp. 139–145). Stara Zagora, Bulgaria.

[28] Rizov, V., Doicheva, A., Mladensky, A., & Keradjiyski, G. (2015). Analysis of a pedestrian bridge with respect to the comfort using the Eurocode. *Annual of the University of Architecture, Civil Engineering and Geodesy*, *XLVIII*(VIII-B), 79–89.

[29] Işik, E. (2025). A study on strengthening RC structural elements with fibers based polymers. *Bitlis Eren University Journal of Science*, *14*(2), 1269–1286. https://doi.org/10.17798/bitlisfen.1675489

[30] Ike, C. (2025). Ritz variational method for the free harmonic vibration solutions of slender beams on two-parameter elastic foundations. *Nigerian Journal of Technology*, *44*(2), 193–201. https://doi.org/10.4314/njt.v44i2.3

[31] Ike, C. (2025). Solving lateral-torsional buckling problems in thin-walled bisymmetric beam using Stodola-Vianelo iteration method. *Nigerian Journal of Technology*, *44*(1), 1–8. https://doi.org/10.4314/njt.v44i1.1

[32] Ike, C. (2024). Stodola-Vianelo iteration method for solving transverse harmonic natural vibration problems of Euler-Bernoulli beams on Winkler foundations. *Iraqi Journal of Civil Engineering*, *18*(2), 73–87. https://doi.org/10.37650/ijce.2024.180206

[33] Lecompte, N., Caratenuto, A., & Zheng, Y. (2025). *Waste animal bone-derived calcium phosphate particles with high solar reflectance*. arXiv. https://doi.org/10.48550/arXiv.2501.18130

[34] Tiwari, S. K., Bystrzejewski, M., Adhikari, A. D., Huczko, A., & Wang, N. (2022). Methods for the conversion of biomass waste into value-added carbon nanomaterials: Recent progress and applications. *Progress in Energy and Combustion Science*, *92*, Article 101023. https://doi.org/10.1016/j.pecs.2022.101023

[35] Hussin, M. H., Abd Latif, N. H., Hamidon, T. S., Idris, N. N., Hashim, R., Appaturi, J. N., Brosse, N., Ziegler-Devin, I., Chrusiel, L., Fatriasari, W., Syamani, F. A., Iswanto, A. H., Hua, L. S., Osman Al Edrus, S. S. A., Lum, W. C., Antov, P., Savov,

V., Lubis, M. A. R., Kristak, L., Reh, R., & Sedliacik, J. (2022). Latest advancements in high-performance bio-based wood adhesives: A critical review. *Journal of Materials Research and Technology*, *21*, 3909–3946. https://doi.org/10.1016/j.jmrt.2022.10.156

[36] Hashin, Z., & Shtrikman, S. (1963). A variational approach to the theory of elastic behaviour of multiphase materials. *Journal of the Mechanics and Physics of Solids*, *11*, 127–140. https://doi.org/10.1016/0022-5096(63)90060-7

[37] Shi, C., Tu, Q., Fan, H., & Li, S. (2016). An interphase model for effective elastic properties of concrete composites. *Journal of Micromechanics and Molecular Physics*, *1*(1), Article 1650005. https://doi.org/10.1142/S2424913016500053

[38] Dong, Z., Quan, W., Ma, X., Li, X., & Zhou, J. (2023). Asymptotic homogenization of effective thermal-elastic properties of concrete considering its three-dimensional mesostructure. *Computers & Structures*, *279*, Article 106970. https://doi.org/10.1016/j.compstruc.2022.106970

[39] Wall, P. (1997). A comparison of homogenization, Hashin–Shtrikman bounds and the Halpin–Tsai equations. *Applications of Mathematics*, *42*(4), 245–257.

[40] Kurukuri, S. (2005). *Homogenization of damaged concrete meso-structures using representative volume elements – Implementation and application to SLang* [Master's thesis, Bauhaus–University Weimar].

[41] Benfrid, A., & Murawski, K. (2025). Thermo-mechanics of eco-concrete beams reinforced with waste pottery. *International Science and Technology Journal*, *37*(2), 1–23. https://doi.org/10.62341/AKBM2379

[42] Lee, T.-F. F., & Cohen, M. D. (n.d.). *Strength and durability of concrete: Effects of cement paste-aggregate interfaces, Part II: Significance of transition zones on physical and mechanical properties of Portland cement mortar* [Technical report]. JTRP.

[43] Luciano, R., & Willis, J. R. (2006). Hashin–Shtrikman based FE analysis of the elastic behaviour of finite random composite bodies. *International Journal of Fracture, 137*, 261–273. https://doi.org/10.1007/s10704-005-3067-z

[44] Aouissi, F., Yang, C.-C., Brahma, A., & Zorkane, O. (2018). Comparison between biphasic and triphasic model for predicting the elastic modulus of concrete. *MATEC Web of Conferences*, *203*, Article 06003. https://doi.org/10.1051/matecconf/201820306003

[45] Shi, C., Tu, Q., Fan, H., & Li, S. (2016). An interphase model for effective elastic properties of concrete composites. *Journal of Micromechanics and Molecular Physics*, *1*(1), Article 1650005. https://doi.org/10.1142/S2424913016500053

[46] Avhad, P. V., & Sayyad, A. S. (2020). On the static deformation of FG sandwich beams curved in elevation using a new higher order beam theory. *Sādhanā*, *45*(1), Article 188. https://doi.org/10.1007/s12046-020-01425-y

[47] Benfrid, A., Bouiadjra, M., Chatbi, M., & Harrat, Z. (2024). Impact of glass nanoparticles on the elastic modulus of concrete. *University of Zawia Journal of Engineering Sciences and Technology*, *2*(2), 182–188. https://doi.org/10.26629/uzjest.2024.16

[48] Ekpraseert, J., Fongkaew, I., Chainakun, P., Kamngam, R., & Boonsuan, W. (2020). Investigating mechanical properties and biocement application of $CaCO_3$ precipitated by a newly-isolated Lysinibacillus sp. WH using artificial neural networks. *Scientific Reports*, *10*(1), Article 16137. https://doi.org/10.1038/s41598-020-73217-7

[49] Ghugal, S. B., & Sayyad, I. I. (2011). Free vibration of thick isotropic plates using trigonometric shear deformation theory. *Journal of Solid Mechanics*, *3*(2), 172–182.

[50] Sayyad, I. I., Chikalthankar, S. B., & Nandedkar, V. M. B. (2013). Bending and free vibration analysis of isotropic plate using refined plate theory. *Bonfring International Journal of Industrial Engineering and Management Science*, *3*(2).

[51] Kaewsit, S., Sompong, K., Pakawanit, P., Akkalatham, W., & Yongsiri, P. (2025). The study of lightweight expanded clay aggregate from industrial waste. *Chiang Mai Journal of Science*, *52*(5), Article e2025061. https://doi.org/10.12982/CMJS.2025.061

[52] Zhang, S., Zhong, Z., Wang, Z., Dai, Y., Niu, D., Liu, J., et al. (2025). A piezoelectric stick-slip actuator utilizing an asymmetric inertial driving foot: Design, analysis and experiments. *Chiang Mai Journal of Science*, *52*(5), Article e2025062. https://doi.org/10.12982/CMJS.2025.062

[53] Chareerat, T., Nuanlert, N., Laorchan, J., Onputta, N., Pranudtaa, A., Rukzon, S., et al. (2025). Effect of aggregate size and void ratio on plant growth in porous concrete-based hydroponic systems. *Chiang Mai Journal of Science*, *52*(5), Article e2025073. https://doi.org/10.12982/CMJS.2025.073

[54] Dechboon, N., Wilai, A., Wilai, P., & Tungyai, T. (2025). Sustainability in celadon glazes using lampang kaolin waste and longan wood ash on the characteristics and heat-resistant properties for sankampang kiln wares. *Chiang Mai Journal of Science*, *52*(4), Article e2025047. https://doi.org/10.12982/CMJS.2025.047

[55] Bello, S., Uthman, T. O., Surgun, S., & Sokoto, A. M. (2025). Characterization, compositional analysis and calorific value of Terminalia ivorensis sawdust, corncob and low-density polyethylene as potential blended feedstock for bio-oil production. *Chiang Mai Journal of Science*, *52*(4), Article e2025056. https://doi.org/10.12982/CMJS.2025.056

[56] Abdulkareem Adil Al-Ani, Hilal, N., Muthusamy, K., Chatbi, M., & Harrat, Z. R. (2025, May). Static and dynamic analysis of bridge decks reinforced with nanoparticles. In M. F. Baran & S. Seydoşoğlu (Eds.), *International Congress on Global Practice of Multidisciplinary Scientific Studies-X*. Liberty Publications.

[57] Benfrid, A., Chatbi, M., Harrat, Z. R., & Bachir Bouiadjra, M. (2025). Selective integration of waste-derived glass nanopowders in structural wall concrete: Improving thermal efficiency and elasto-mechanical properties for sustainable construction. *Periodica Polytechnica Civil Engineering*, *69*(3), 954–965. https://doi.org/10.3311/PPci.39913

[58] Harrat, Z. R., Chatbi, M., Krour, B., Amziane, S., Bouiadjra, M. B., Hadzima-Nyarko, M., Radu, D., & Işık, E. (2024). Bending analysis of nano-Fe_2O_3 reinforced concrete slabs exposed to temperature fields and supported by viscoelastic foundation. *Advances in Concrete Construction*, *17*(2), 111–126. https://doi.org/10.12989/acc.2024.17.2.111

[59] Lakhder, M., Benfrid, A., Bachir Bouiadjra, M., Chatbi, M., Harrat, Z. R., & Benbakhti, A. (2025). The mechanical bending behavior of a new metal alloy nano-reinforced plate incorporating tungsten nanoparticles. *NIPES – Journal of Science and Technology Research*, *7*(3), 423–440. https://doi.org/10.37933/nipes/7.3.2025.1682

[60] Chatbi, M., Harrat, Z. R., Benatta, M. A., Krour, B., Hadzima-Nyarko, M., Işık, E., Czarnecki, S., & Bouiadjra, M. B. (2023). Nano-clay platelet integration for enhanced bending performance of concrete beams resting on elastic foundation: An analytical investigation. *Materials*, *16*(14), Article 5040. https://doi.org/10.3390/ma16145040

[61] Ahmed, B., Mohamed, A., Baghdad, S., & Abdelmoutalib, B. (2025). First-principles study of the structural, electronic, and elastic properties of hydride perovskites $XCaH_3$ (X = Na, K, Rb, Cs) under pressure. *Veredas do Direito*, *22*(2), Article e3223. https://doi.org/10.18623/rvd.v22.n2.3223

[62] Bouchehit, H., Torkia, H., Kadid, A., & Benfrid, A. (2025). Comparative seismic analysis of cylindrical and rectangular oil tanks: Effects of wall thickness under soil–structure–fluid interaction. *Veredas do Direito*, *22*(2), Article e3224. https://doi.org/10.18623/rvd.v22.n2.3224

[63] Ahmed, B., Hafida, D., Djihad, R., & Abdelmoutalib, B. (2025). Flexural performance of concrete beams incorporating granite waste. *Veredas do Direito*, *22*(2), Article e3155. https://doi.org/10.18623/rvd.v22.n2.3155

[64] Yerkrou, A., Benfrid, A., Krour, B., & Bouiadjra, M. B. (2025). A programming model for analyzing the mechanical and thermal buckling behavior of eco-concrete panels incorporating recycled waste materials (glass and red bricks). *Veredas do Direito*, *22*(2), Article e3117. https://doi.org/10.18623/rvd.v22.n2.3117

[65] Abdelmoutalib, B., Murawski, K., & Samir, B. (2025). Thermal instability of a polymer panel reinforced with glass particulates. *ISPEC Journal of Science Institute, 4*(2), 210–215. https://doi.org/10.5281/zenodo.18062068

[66] Benfrid, A. (2026). *Prediction of thermal and mechanical properties of eco-concretes using a biphasic homogenization approach*. Zenodo. https://doi.org/10.5281/zenodo.19322922

[67] Belmahi, S., Benfrid, A., Klouche Djedid, I., Guergour, R., & Djakhdane, N. (2026). Influence of acidic and alkaline environments on the mechanical properties of cement mortars. *Periodica Polytechnica Civil Engineering*, *70*(1), 315–326. https://doi.org/10.3311/PPci.42312

[69] Benfrid, A. (2026). The elastomechanical properties of concrete expanded with aluminum nano-inclusions. *Journal International Review of Research Studies, 1*(02), 1–9. https://doi.org/10.66104/gkkj0g48

[70] Khetir, H., Benfrid, A., Bachir Bouiadjra, M., & Melati, L. (2026). Contribution to the mechanical performance of a simply supported lightweight concrete beam reinforced with bio-sourced nanocomposites. *Revista Brasileira de Engenharia de Biossistemas, 19*. https://doi.org/10.18011/bioeng.2025.v19.1293

[71] Chatbi, M., Harrat, Z. R., Benatta, M. A., Krour, B., Hadzima-Nyarko, M., Işık, E., Czarnecki, S., & Bouiadjra, M. B. (2023). Nano-clay platelet integration for enhanced bending performance of concrete beams resting on elastic foundation: An analytical investigation. *Materials*, *16*(14), Article 5040. https://doi.org/10.3390/ma16145040

[72] Harrat, Z. R., Achour, A., Chatbi, M., Hadzima-Nyarko, M., & Işık, E. (2026). Modelling the dynamic response of clay nanoparticle-modified concrete beams resting on two-parameter elastic foundations. *Modelling*, *7*(2), Article 64. https://doi.org/10.3390/modelling7020064

[73] Zahafi, A., Hadid, M., & Bencharif, R. (2024). Lumped parameter model for vertical vibrations of surface circular foundations on nonhomogeneous soil. *World Journal of Engineering*, *21*(4), 632–653. https://doi.org/10.1108/WJE-01-2023-0012

[74] Bencharif, R., Zahafi, A., Mezouar, N., & Hadid, M. (2023). Time-domain implementation of soil-structure interaction analysis techniques with frequency-dependent impedance functions. *Algérie Équipement*, *69*, 1–20.

[75] Chatbi, M., Lozančić, S., Harrat, Z. R., & Hadzima-Nyarko, M. (2026). Computational models for the vibration and modal analysis of silica nanoparticle-reinforced concrete slabs with elastic and viscoelastic foundation effects. *Modelling*, *7*(1), Article 8. https://doi.org/10.3390/modelling7010008

[76] Chatbi, M., Harrat, Z. R., Ghazoul, T., & Bachir Bouiadjra, M. (2022). Free vibrational analysis of composite beams reinforced with randomly aligned and

oriented carbon nanotubes, resting on an elastic foundation. *Journal of Building Materials and Structures*, *9*(1), 22–32. https://doi.org/10.34118/jbms.v9i1.1895

[77] Bencharif, R., Hadid, M., & Mezouar, N. (2020). Hybrid BEM-TLM-PML method for the dynamic impedance functions calculation of a rigid strip-footing on a nearly saturated poroelastic soil profile. *Engineering Analysis with Boundary Elements*, *116*, 31–47. https://doi.org/10.1016/j.enganabound.2020.03.001

[78] Tebbouche, M. Y., Ait Benamar, D., Hassan, H. M., et al. (2022). Characterization of El Kherba landslide triggered by the August 07, 2020, Mw = 4.9 Mila earthquake (Algeria) based on post-event field observations and ambient noise analysis. *Environmental Earth Sciences*, *81*, Article 46. https://doi.org/10.1007/s12665-022-10172-8

[79] Benfrid, A. (2026, March). *Évaluation théorique des propriétés effectives des bétons environnementaux: Une étude comparative des modèles d'homogénéisation* [Unpublished manuscript].

[80] Sid Ahmed, M., Benfrid, A., Benosman, A. S., Hacini, M., Mouli, M., Taleb, O., & Badache, A. (2026). Analysis of thermally treated "plastic-pozzolanic" modified mortars and their mechanical properties. *Zastita Materijala*. https://doi.org/10.62638/ZasMat1595

[81] Sid Ahmed, M., Hacini, M., Benosman, A. S., et al. (2026). Development of eco-friendly composite mortars for the circular economy and sustainable construction: Rheological, thermo-mechanical, durability characterization, and environmental impact assessment (LCA). *Circular Economy and Sustainability*, *6*, Article 80. https://doi.org/10.1007/s43615-026-00747-z

[82] Turan, F., & Benfrid, A. (2025, December). *Free vibration of higher-order shear deformable porous orthotropic beams* [Paper presentation]. Engineering and Artificial Intelligence in Achieving Sustainable Development for State Building Conference, Libya.

[83] Benfrid, A. (2025, October 4–7). *The free vibration of a building's raft foundation reinforced with short steel fibers* [Paper presentation]. 15th International Mardin Artuklu Scientific Researches Conference, Mardin, Türkiye.

[84] Benfrid, A., & Turan, F. (2025, December). *Eco-friendly concrete: Thermal transfer study of panels with low concentrations of recycled cardboard* [Paper presentation]. Engineering and Artificial Intelligence in Achieving Sustainable Development for State Building Conference, Libya.

[85] Abdelmoutalib, B., Murawski, K., & Samir, B. (2025). Thermal instability of a polymer panel reinforced with glass particulates. *ISPEC Journal of Science Institute*, *4*(2), 210–215. https://doi.org/10.5281/zenodo.18062068

[86] Mladenov, K., & Doicheva, A. (2009). On some illustrative potentialities of simply supported beams. In *Proceedings of the 11th National Congress on Theoretical and Applied Mechanics* (pp. 1–8). Borovets, Bulgaria. http://nctam.imbm.bas.bg/index.php/nctam/nctam2009/paper/viewFile/127/43

[87] Mladenov, K., & Doicheva, A. (2009). Flexural-torsional buckling of an off-centre supported beam. *Annual of the University of Architecture, Civil Engineering and Geodesy*, *XLIV*(V), 103–114.

[88] Doicheva, A. (2011). Exact solution for a beam on off-center spring supports. *Journal of Theoretical and Applied Mechanics*, *41*(2), 69–82.

[89] Doicheva, A. (2016). T-shaped frame critical and post-critical analysis. *Journal of Theoretical and Applied Mechanics*, *46*(1), 65–82.

[90] Mladenov, K., & Doicheva, A. (2016). Critical and post-critical analysis of water tower with conical tank. *Annual of the University of Architecture, Civil Engineering and Geodesy*, *49*(2), 63–76.

[91] Mladenov, K., & Doicheva, A. (2008). Bending-torsional buckling of a beam on elastic rotational springs. *Civil Engineering*, (6), 2–7.

[92] Doicheva, A., & Mladenov, K. (2005). On some dynamic characteristics in the analysis of building structures. In *Proceedings of the Scientific Conference with International Participation* (Vol. 1, pp. 139–145). Stara Zagora, Bulgaria.

[93] Doicheva, A. (2024). Shear force of interior beam–column joints under symmetrical loading with two transverse forces on the beam. *Buildings*, *14*(9), Article 3028. https://doi.org/10.3390/buildings14093028

[94] Doicheva, A. (2024). Shear force in RC internal beam-column connections for a beam loaded with a transverse force occupying different possible positions. *The Eurasia Proceedings of Science, Technology, Engineering & Mathematics*, *29*, 128–144. https://doi.org/10.55549/epstem.1563437

[95] Doicheva, A. (2024). Alteration of the shear force in an internal beam-column joint during the initiation and growth of a crack in a cantilever beam. *Procedia Structural Integrity*, *66*, 433–448. https://doi.org/10.1016/j.prostr.2024.11.096

[96] Doicheva, A. (2025). Repercussions on the shear force of an internal beam–column connection from two symmetrical uniformly distributed loads at different positions on the beam. *Engineering Proceedings*, *87*, Article 85. https://doi.org/10.3390/engproc2025087085

[97] Doicheva, A. (2025). Horizontal shear force in RC internal beam-column connection at initiation and crack growth from linearly distributed load on a cantilever beam. *Procedia Structural Integrity*, *72*, 235–242. https://doi.org/10.1016/j.prostr.2025.08.098

[98] A new approach for studying plaster beam bending based on DISS Algerian (nano-short-bio-fibres). (2025). *Modern Journal of Health and Applied Sciences*, *2*(1), 43–58. https://doi.org/10.70411/MJHAS.2.1.2025183

[99] Benfrid, A., Bouiadjra, M. B., Harrat, Z. R., & Saoudi, F. (2025, April). *Thermal insulation using bio-based concrete made from apricot kernels* [Paper presentation]. First National Conference on Mechanical Applications (CNAM1 2025), Centre Universitaire Maghnia, Algeria.

[100] Benfrid, A., Bouiadjra, M. B., & Saoudi, F. (2025, April 22). *Enhancing thermal efficiency of bio-concrete with wheat straw nanofibers: A sustainable approach for energy-efficient buildings* [Paper presentation]. 2nd Online National Conference on Materials Physics (ONCMP'25), El Tarf, Algeria.